Hot Processing of Powder Metallurgy and Wrought Ti-6Al-4V Alloy with Large Total Deformation: Physical Modeling and Verification by Rolling

MAREK WOJTASZEK, GRZEGORZ KORPAŁA, TOMASZ ŚLEBODA, KRYSTIAN ZYGUŁA, and ULRICH PRAHL

The influence of the total deformation amount on the microstructure and selected properties of Ti-6Al-4V alloy was determined in this study. Multi-axis compression tests on the MaxStrain module were performed to obtain large strains. Starting material for the research was obtained by the powder metallurgy (PM) route. Plastically processed cast alloy of the same chemical composition as PM alloy was also tested as reference material. The tests were performed with the cooling of samples between successive deformation stages, which allowed for the simulation of the temperature drop occurring during industrial processes. The multi-stage deformation ability of PM Ti-6Al-4V alloy without decohesion was confirmed. It has also been shown that the application of increasing total strain at a controlled temperature changes the samples resulting in the refinement of the microstructure and leads to the fragmentation of lamellae. The results obtained from MaxStrain tests were verified by multi-stage hot-rolling tests. Defect-free products were obtained, whose good quality was confirmed by the microstructural observations as well as by the investigations of their properties. The results of the rolling tests confirmed the possibility of hot processing of Ti-6Al-4V alloy compacts in industrial conditions, applying large total strain.

I. INTRODUCTION

THE most common group of titanium alloys is dual-phase alloys. They are mainly used in the aviation, automotive, defense, shipbuilding, medicine and many other branches of industry.[1–5] The attractiveness of these materials is primarily due to the properties of titanium, among which are low density, high strength, resistance to cracking, corrosion and fatigue strength.[2,6] Some of the titanium alloys maintain high strength under dynamic loads[1,7,8]; others are biocompatible and resistant to corrosion in a biological environment, which allows their use in the manufacturing of implants.[9–13] The significant disadvantages of titanium and its alloys include low thermal conductivity, difficulties in their machining[14–16] and relatively high

production costs.[1,17–19] At present, a semi-finished product in the form of the processed cast material is commonly used for the production of highly responsible titanium alloy structural parts.[1] However, attempts are being made to replace it by using the powder metallurgy methods,[9,17,20,21] because it reduces production costs. Cost reduction can be achieved by using inexpensive initial material, implementing waste-free processes and conducting processes at lower temperatures compared to the methods based on casting. Among the downsides resulting from the use of powder metallurgy technology for the production of titanium alloys, the most important is the occurrence of porosity and limitation of the size and shape of the products.[22] When using initial materials in the form of elemental powders, there is also the risk of inhomogeneity of the chemical composition in the volume of the products. However, the occurrence of these faults can be prevented by proper selection of the method of mixing the powders and by including hot processing of the semi-finished products in the production chain.

Among the dual-phase titanium alloys, Ti-6Al-4V is the most widely applied. In addition to titanium-specific advantages, it also exhibits heat resistance, good weldability and good ductility.[1] Additionally, good formability of the investigated material means that under

---

MAREK WOJTASZEK, TOMASZ ŚLEBODA and KRYSTIAN ZYGUŁA are with the Faculty of Metals Engineering and Industrial Computer Science, AGH University of Science and Technology, Al. A. Mickiewicza 30, 30-059 Kraków, Poland. Contact e-mail: mwojtasz@metal.agh.edu.pl GRZEGORZ KORPAŁA and ULRICH PRAHL are with the Institut für Metallformung, Technische Universität Bergakademie Freiberg, Bernhard-Von-Cotta Str. 4, 09-599 Freiberg, Germany.

appropriately selected conditions it can be processed in commonly used metal-forming processes.[23] Therefore, if responsible structural parts are produced in this way, it is necessary to know the combinations of thermomechanical parameters that lead to obtaining products that are free of defects with an assumed geometry as well as to obtaining a microstructure that guarantees high mechanical and functional properties.[24,25] While for Ti-6Al-4V alloy produced in the conventional route this knowledge is well systematized and available, in the case of semi-finished products made of elemental powders, the data collected in the literature are incomplete.[26,27] However, the analysis of the literature indicates that in recent years advanced research has been carried out on the possibility of using the semi-products obtained by PM technology as the stock for processing titanium alloys. They are implemented both by the scientific institutes, where the results of the investigations were published for example in References 26, 28 through 31, and by research and development units cooperating with commercial companies, dealing with the design and production of parts obtained from these materials.[2,5,32,33]

Currently, many of the metal-forming processes, such as multi-axis forging, drawing or rolling, can be carried out with large total strains, obtained as a result of the application of the many successive single deformations. Hot forming of titanium alloys under conditions of accumulation of deformation allows not only for a significant change in the shape of the feedstock, but also for deep processing leading to the refinement of the microstructure and ultimately to obtaining specific, usually anisotropic properties of the products. For this reason, it is necessary to understand the impact of the total amount of the deformation in the processed material on its properties. Commonly used plastometric tests are fully sufficient to describe the rheology of the material and to determine favorable ranges of the temperature and strain rate combinations; however, their results do not reflect the effects of strain accumulation. Therefore, physical modeling of the processes carried out under conditions of deep processing requires the use of such a method, which allows applying a large amount of total strain under controlled conditions. One of the techniques that can be used for this purpose is a multi-axis compression test, carried out using the MaxStrain module. MaxStrain tests allow conducting deformation in two axes, while the deformation in the third axis is blocked, which ensures that almost the entire volume of the material is maintained in the deformation zone.[34] The principle of the MaxStrain test is shown in Figure 1. The module consists of a rigid frame and clamps enabling the sample to rotate around its long axis by 90 deg. The deformation is carried out using two anvils moving in opposite directions. The surface A in the diagram schematically shows the idea of blocking the flow of the material in the direction of the O axis. The amount of deformation obtained in a single compression operation is usually from 0.3 to 0.5. In the next stage of the MaxStrain test, 90 deg rotation around the long axis of the sample is performed, and the compression process is repeated. Repeating the sequence
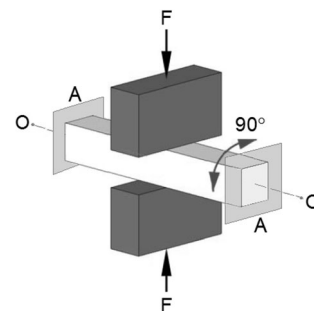

Fig. 1—Schematic representation of the MaxStrain test.

the assumed number of times, the total deformation of up to 30 can be achieved for the processed material, without its decohesion.

MaxStrain tests allow to obtain the effect of fragmentation of the microstructure to the ultra-fine or nanocrystalline level. This is one of the methods resulting in high deformation accumulation in the processed material (severe plastic deformation, SPD) along with modification of its microstructure.[34–36] In this case, the sequence of deformations is usually realized at a constant temperature, which is appropriate to obtain the grain refinement effect without the risk of decohesion of the tested material. However, the MaxStrain module also allows to perform physical simulation of the metal-forming processes that are realized in many single deformations and with an application of large total strain, such as a multi-stage forging or multi-pass rolling.[34,37] In this case, if the modeled process is carried out in non-isothermal conditions, the test should take into account the controlled drop in the temperature of the material, which can be realized using the MaxStrain module. It can be determined whether during the realization of the modeled process at industrial conditions it is possible to perform the assumed total strain without the material decohesion. The assessment of the fragmentation of the microstructure and determination of the properties of the investigated material lead to the supplementation of knowledge developed on the basis of commonly used plastometric tests conducted at the constant deformation values.

The aim of this study was determining the effect of the total strain on the microstructure and selected properties of Ti-6Al-4V alloy compacts made from the mixture of elemental powders as well as comparing the achieved knowledge with the results obtained for the plastically processed cast alloy tested under the same conditions. As the initial materials for manufacturing the compacts, relatively cheap elemental powders were used to reduce the cost of manufacturing products and give a real opportunity to implement the proposed technology, which was reported for example in References 38 and 39. The scope of the study included multi-axis compression tests using the MaxStrain module and verification of the obtained results basing on multi-stage hot-rolling tests. It was assumed that the tests using the MaxStrain module could be useful to supplement the knowledge about the tested alloy. This approach, despite its effectiveness, is currently not widely used for the analysis

of the materials obtained by the powder metallurgy route. An analysis of the microstructure evolution and estimation of the investigated material mechanical properties, both at the initial state and after deformation, was performed. The basis for the possible use of the research results in the industrial conditions was prepared. Since the currently used feedstock for manufacturing of Ti-6Al-4V alloy products is obtained by a commonly used casting process, it was also assumed that the comparison of the results for such material with that obtained from elemental powders will allow for the assessment of PM alloy quality.

II. EXPERIMENTAL PROCEDURE

A. Initial Materials for Testing

The investigated material was manufactured by hot pressing of an elemental powder mixture. The Ti-6Al-4V alloy selected for the comparison with PM alloy was a hot-rolled cast alloy of the same chemical composition as the PM material. The hot-rolled cast alloy was rod shaped with 50.8 mm diameter. This material is currently widely used both for the production of structural parts by machining and as the stock for the hot processing.[1]

B. Manufacturing of PM Ti-6Al-4V Alloy

As the initial materials for the production of the Ti-6Al-4V alloy compact, elemental powders of titanium, aluminum and vanadium were used. Vanadium and titanium powders with irregular particle shape and size < 150 μm and spheroidal aluminum powder with particle size < 45 μm were used. It was assumed that with a properly selected mixing method, inserting the aluminum particles on the surfaces of the particles of the remaining components of the mixture should take place.

The mixing process was carried out in a ceramic container using tungsten carbide balls as milling medium. The powders were mixed for 120 minutes at a rotation speed of about 55 rpm.

The hot pressing of the mixtures was carried out under conditions favorable for the consolidation of powder particles, homogenization of the chemical composition as well as for the obtaining high relative density of the products. It is well known that both self-diffusion of titanium and other alloying elements in titanium are four orders of magnitude higher in the case of β phase than in the case of α phase.[2,40,41] The results presented by Ivashin *et al.*[41] show that conducting the process with appropriate pressure for a suitable time and applying the temperature in the β phase range lead to homogenization of the material and promote the elimination of the porosity. Considering the above, the feedstock designed for further plastic working was made of a hot compacted powder mixture. The compacting process was carried out for 3 hours at the temperature of 1200 °C under 25 MPa pressure. To prevent oxidation, a protective argon atmosphere was applied.

1. Chemical composition of compacts

To perform a chemical analysis of the compacts (Table I) the following laboratory equipment was used: A LECO R016 apparatus for oxygen determination, N-Leco TN14 apparatus for nitrogen determination, and Niton XL3t analyzer (based on X-ray fluorescence spectroscopy) for determination of the content of other elements.

C. Multi-axis Compression Tests on MaxStrain Module

Physical modeling of the hot-forming processes with large total strain was performed using MaxStrain module, working with the thermomechanical simulator Gleeble 3800 (Dynamic Systems Inc., Poestenkill, NY). Direct resistance heating of samples allowed for precise control of their temperature during testing. The flow of the material towards the long axis direction was blocked during testing; therefore, almost the entire volume of the material was maintained in the deformation zone. Rotating the sample by 90° after each successive compression operation caused the material to flow perpendicular to the direction of the previous deformation.

1. Assumptions for MaxStrain tests

At the initial stage of MaxStrain tests the possibility of multi-stage deformation of the alloy obtained by powder metallurgy without decohesion was confirmed. Then, multi-stage compression tests of the PM alloy and plastically processed cast alloy were carried out, using the same conditions. Between successive deformation stages, the samples were cooled down, which allowed for the simulation of the temperature drop occurring during hot forming in industrial conditions. Since the microstructure of the plastically processed cast alloy in as-received condition was globular and fine-grained, a preliminary heat treatment was applied, which led to the reconstruction of the microstructure to the lamellar form consisting of α phase lamellae in β phase matrix, located inside the large-sized primary grains of β phase. In the next steps, the samples were compressed multi-axially with increasing total strain and with a controlled temperature change, in the result of which the original structure of the material was rebuilt, with a level of fragmentation comparable to the initial state. The same heat treatment and deformation sequences were performed for the alloy obtained by powder metallurgy.

The adopted assumptions allowed determining the impact of the method of manufacturing of the Ti-6Al-4V alloy as well as the effect of the total strain on the microstructure and selected properties of the tested materials.

2. MaxStrain multi-axis compression tests

The 40-mm-long samples with a cross-section of 10 mm × 10 mm were used for testing. Figure 2 shows how to mount the sample (Figure 2(a)) and the sample during the heating inside the MaxStrain module chamber (Figure 2(b)). The contact surfaces of samples and holders were covered with a lubricant, which facilitated

the current flow and prevented from welding of these components during the tests.

Table II presents the MaxStrain test parameter combinations that were carried out in the same way for PM semi-products and for plastically processed cast samples. The samples were heated up to 1000 °C with a heating rate of 4 °C s^{-1} and held at this temperature for 6 minutes, and then the assumed sequence of deformations was carried out. A strain of 0.3 in one compression operation was assumed. The tests were performed using 5, 8 and 12 single compression operations, respectively. A total strain value for the samples in the first variant was 1.5, in II variant was 2.4 and in III variant was 3.6. Between subsequent deformations, the intervals were introduced during which the samples were cooled. In variants I and II, the interval time was 10 seconds and the temperature of the samples reduced by 20 °C. During the implementation of the III variant, at its last stage (deformations from 9 to 12), the time between successive deformations was shortened to 5 seconds, and temperature drops were reduced to 5 °C. Compression operations were carried out at a constant strain rate of 1 s^{-1}. The anvil temperature was 500 °C. After the tests, the samples were cooled down with compressed air.

D. Hot Rolling of Ti-6Al-4V Alloy

The possibility of hot forming of PM alloy with large total strain at the conditions obtainable on an industrial processing line required confirmation. Therefore, hot-rolling tests of Ti-6Al-4V alloy were carried out. As a feedstock for rolling the material obtained by powder metallurgy route and for comparison, a plastically processed cast material was used.

1. Preparation of the feedstock for the rolling process

Since the geometry of PM semi-products (diameter 78 mm, height approximately 45 mm) was unsuitable as the feedstock for the rolling process, it was necessary to pre-process it. Therefore, the compacts were kept for 15 minutes in the furnace heated up to the temperature of 1000 °C and then forged on a 10 MN hydraulic press, giving them the shape of a rod with a about 41 mm diameter and 85 mm length.

2. Hot-rolling tests

A semi-industrial stand operating as a three-high rolling mill enabled processing small samples that could be made of hot-pressed compacts. The rolling mill enables the process to be carried out with a maximum pressure of 600 kN, a torque of up to 60 kNm and a rolling speed in the range of 0.1 to 2.5 m s^{-1}. The values of true strain assumed during the rolling in the subsequent passes are summarized in Table III. They were

determined taking into account the effects occurring during the rolling process, which had an impact on the geometry of the deformation zone (*i.e.*, elastic deformation of rolls).

The preliminary assessment of the technical possibilities of forming the examined alloy at the experimental-industrial stand was carried out for the feedstock obtained by PM technology. The sample was heated to the temperature of 1000 °C, and then it was subjected to multi-pass rolling, which began with the roll pass (roll groove) number 1 (Table III) and was continued in subsequent roll passes. The sample temperature was monitored by the pyrometers. After passing through the roll pass number 5, the temperature dropped below 800 °C. Continued rolling in the sequence presented in Table III led to decohesion of the material due to excessive cooling and a decrease of the ductility. Considering the above, the hot-rolling process was divided into two stages (Figure 3). The first stage (Table III—stage I-1 to I-5) was aimed at pre-processing the feedstock and giving the appropriate initial geometry. Then, the samples were heated up again and then rolled to the final geometry (Table III—stage IIA1, B1 to IIA4, B7). Because it was confirmed based on MaxStrain tests, as a result of properly designed and performed heat treatment, the microstructure of the feedstock was rebuilt, and the effects of previous deformation were removed. Hence, it was assumed that the microstructure of the feedstock depended mainly on the deformation during the second stage of rolling.

At the first stage, the feedstock was heated up to 1000 °C for 15 minutes and then rolled in five passes, using roll grooves ordered in the sequence from 1 to 5 (Table III: I-1 to I-5). The rod of the cross-sectional area in the form of an ellipse with a large axis of 29.65 mm was obtained. The total strain was about 2.9. The rod was cooled in air and then cut into two parts, which allowed the process to be carried out with different total strains, using the material with the same history of deformation. In the second stage, both parts of the rod were heated for 15 minutes at 1000 °C. Then, one part was rolled in four passes (Table III: IIA-1 to IIA-4), using roll passes ordered in the sequence from 6 to 9. As a result, the rod of the cross-sectional area in the form of an ellipse with a large axis of 17.35 mm was manufactured. The total strain given during this stage was about 2.1. The second part of the rod was rolled in the same way and additionally in roll grooves numbered from 10 to 12 (Table III: IIB-1 to IIB-7). The rod of the cross-sectional area in the form of the circle with a diameter of 7.7 mm was obtained, and the total strain was about 3.5. After the rolling process, both products were cooled down in air.

Table I. Result of the Analysis of the Chemical Composition of Compacts

Chemical Element	Al	V	Fe	Cu	Mn	Cr	O	N	Ti
Content (Wt Pct)	5.60	4.15	0.33	0.008	0.090	0.096	0.025	0.0017	Bal.

3. Testing of samples

To analyze the microstructure of unprocessed and deformed Ti-6Al-4V alloy samples, a Leica DM4000M light microscope (Leica Microsystems GmbH, Wetzlar, Germany) was used. Selected cross-sections of the samples were ground, polished and etched in two stages (first stage: 6 pct HF + 96 pct H_2O, second stage: 2 pct HF + 2 pct HNO_3 + 96 pct H_2O). The observations of the microstructure using scanning microscopy were performed on a Hitachi TM-3000 microscope (Hitachi Ltd, Tokyo, Japan). The tests of the mechanical properties included tensile tests (Zwick-Roell GmbH & Co. KG, Ulm, Germany) and Vickers hardness tests (Zwick tester, Zwick GmbH, Ulm, Germany). For the tensile test, the samples with a diameter of 4 mm were cut out from hot-rolled wires in the direction of the rolling process. Vickers tests were conducted under a load of 19.6 N.
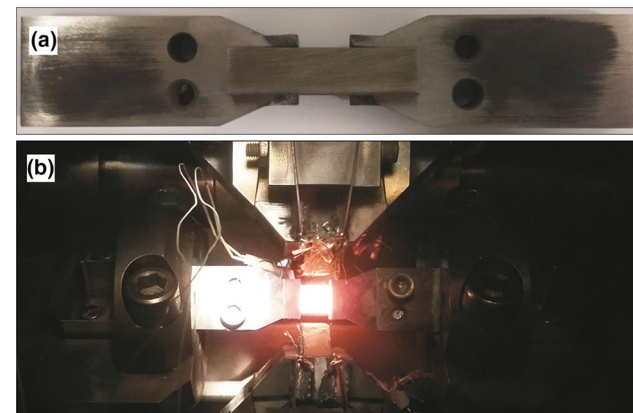
Fig. 2—(*a*) Sample and method for fixing in MaxStrain module holders; (*b*) sample during the test.

III. RESULTS

A. *Characteristics of the Materials Obtained from Ti-6Al-4V Alloy*

The microstructure of the PM semi-products manufactured by the hot compacting of the elemental powder mixture at the temperature of 1200 °C (Figure 4(a)) showed a lamellar character, consisting of massive lamellae of α phase (light phase) in the matrix of β phase (dark phase) and continuous precipitates of α phase located on the primary boundaries of β phase grains. The average content of phases was measured on

Table II. The Conditions of MaxStrain Multi-axis Compression Tests

Test Variant	Total Number of Compression Operations	Strain in One Compression Operation	Time Between Successive Deformation Stages (s)	Decrease in the Sample Temperature Between Operations (°C)	Total Strain in the Sample During the Test
I	5	0.3	10	20	1.5
II	8				2.4
III	12		10 and 5	20 and 5	3.6

Table III. Values of the True Strains Assumed During the Rolling in Subsequent Rolling Passes

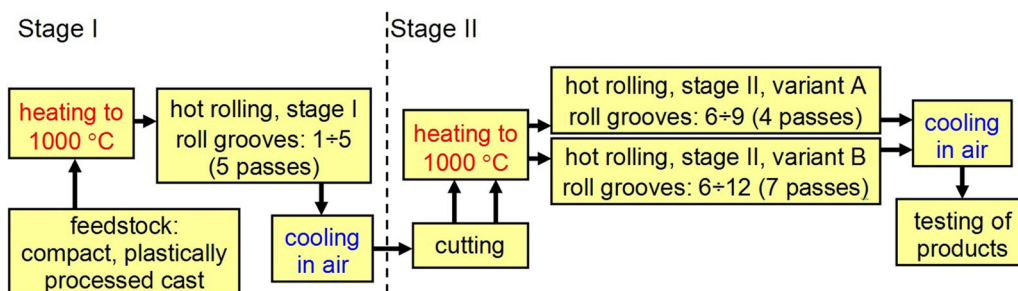| No. of Roll Grooves	1	2	3	4	5	6	7	8	9	10	11	12
Stage and Order of the Pass	I-1	I-2	I-3	I-4	I-5	IIA-1 IIB-1	IIA-2 IIB-2	IIA-3 IIB-3	IIA-4 IIB-4	IIB-5	IIB-6	IIB-7
Roll Groove Geometry	oval	square	oval	square	oval	circle	oval	circle	oval	circle	oval	circle
True Strain	0.66	0.46	0.67	0.48	0.65	0.51	0.60	0.44	0.57	0.40	0.55	0.40

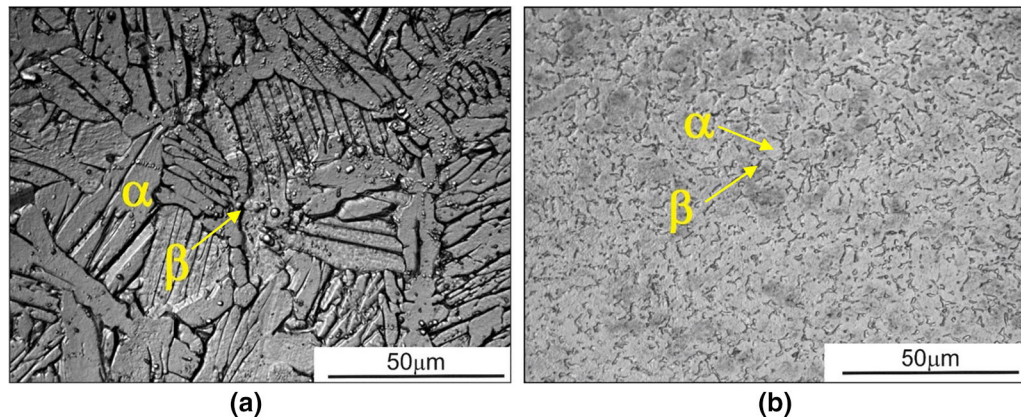Fig. 3—Schematic representation of the hot-rolling test.

Fig. 4—Microstructure of Ti-6Al-4V alloy: (*a*) compact; (*b*) plastically processed cast alloy. The cross-section, etched.

PM Ti-6Al-4V alloy micrographs, using Leica Application Suite 4.8 software. The α and β phase fields were calculated as 91 and 9 pct, respectively.

The microstructure of the standard Ti-6Al-4V alloy rod, produced by casting and hot rolling, in as-delivered condition showed a globular, fine-grained microstructure, consists of equiaxed grains of α phase and the grains of β phase located on the boundaries of the grains of α phase (Figure 4(b)).

The relative density of the compacts was determined, which was 99.4 $\pm$ 0.14 pct. The yield stress $R_{0.2}$ determined in the tensile test of the compact was 950 MPa, and the ultimate tensile strength R_m was 1022 MPa. In the case of the plastically processed cast alloy, the values $R_{0.2}$ = 978 MPa and R_m = 1017 MPa were obtained. It was also found that the ductility of the compact was significantly lower. The elongation value of the compact was A = 5.9 pct and that of the cast was 13.5 pct. The hardness of the powder compact was 338 HV_2 and was higher than that determined for the plastically processed cast alloy, which was 317 HV_2.

B. *MaxStrain Test Results and Characteristics of Deformed Samples*

The changes in the temperature of samples, as well as the values of the forces necessary to implement the assumed strain sequences, were measured during the tests. Figure 5 shows the examples of the results obtained for a test variant involving 12 single compression operations. The start of the mechanical part of the test at the temperature of 1000 °C and its realization with the cooling between successive deformations by 20 °C led in the initial stage of deformation to an increase in the maximum values of subsequent force peaks in relation to the decrease of the temperature of the sample. During subsequent compression operations, carried out at a temperature < 900 °C, the greater increase in the values of forces necessary to obtain successive deformations were observed. To compensate this effect, and to prevent the sample decohesion, when performing the MaxStrain test in the variant involving a sequence of 12 deformations, the last four operations were carried out with reducing the time between successive deformations and reducing the temperature changes of the material (Table II). As a result, the tests at the temperature of 840 °C were finished, and the increase in forces needed to implement subsequent deformations was limited. It was also observed that during MaxStrain tests of PM material (Figure 5(a)), the peaks of the forces were slightly smaller compared to the parameters recorded for the plastically processed cast alloy (Figure 5(b)).

Preliminary assessment of the quality of samples subjected to MaxStrain tests did not reveal any defects on their surfaces indicating decohesion. The samples were prepared to observe the microstructure and to determine properties in the same zone (Figure 6), which allowed for the comparison of test results obtained for different initial materials and with a different history of their total strain.

C. *Microstructural Analysis*

The microstructure of the plastically processed cast alloy in as-delivered condition was fine-grained and globular (Figure 7(a)). Subjecting the samples made from this material to heat treatment, which consisted of heating up to 1000 °C, holding this temperature for 6 minutes without deformation and cooling with compressed air, resulted in a lamellar character of the microstructure. The microstructure consisted of α-phase lamellae located in the β matrix, distributed inside the large primary β phase grains (Figure 7(b)). As a result of increasing the total strain with simultaneous, controlled changes in the temperature, the microstructure gradually returned to its original state (Figures 7(c) through (f)). The microstructure of the compressed samples to a total strain of 1.5 was heterogeneous. Both lamellae of the α phase and the β phase, as well as equiaxed grains of the α phase, were observed. Increasing the value of total strain led to the fragmentation of the lamellae (Figures 7(c) through (f)). The application of total strain of 3.6 resulted in obtaining a globular microstructure with fine grains, similar to those observed in the initial material (Figures 7(e) and (f)).
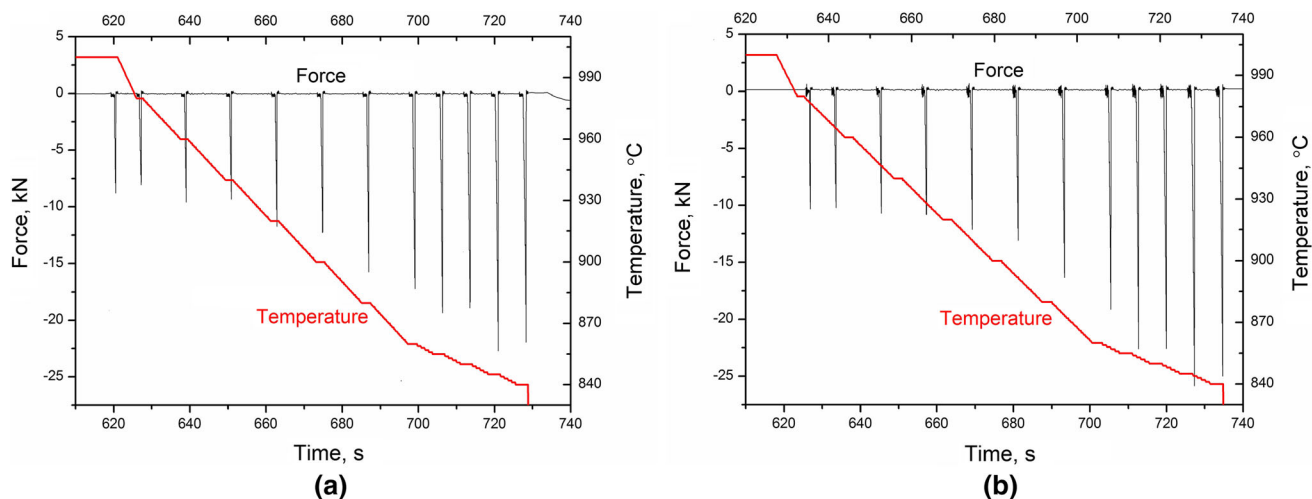
Fig. 5—Characteristics of force and temperature changes during MaxStrain tests carried out with a total strain of 3.6. The samples were obtained by (*a*) powder metallurgy route; (*b*) rolling of the cast alloy.
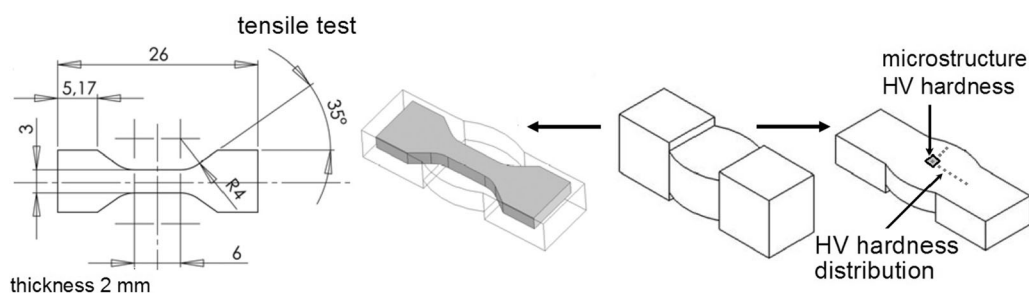

Fig. 6—Method of cutting and machining of the samples after MaxStrain tests.

At the initial state, compacts made of Ti-6Al-4V alloy had a lamellar microstructure composed of short, massive α phase lamellae located inside the β phase matrix, surrounded by massive α phase precipitations formed at the boundaries of the primary β/β grains (Figure 8(a)). Subjecting the compacts to the heat treatment caused changes in the microstructure, which led to obtaining much smaller α phase lamellae and reducing the thickness of these phase precipitations at the primary boundaries of the β phase grains (Figure 8(b)). Applying the deformation and increasing its value in the MaxStrain tests led to the fragmentation of the microstructure (Figures 8(c) through (f)). The reconstruction of the microstructure to a globular form has already begun at total strain of 1.5 and occurred locally. Fragmentation of the α phase was observed in the areas inside of some of the primary β phase grains and at their boundaries, while neighboring grains still showed a lamellar microstructure (Figure 8(c)). This effect occurred because of the favorable orientation of α phase lamellae in individual grains in relation to cyclically variable directions of force in subsequent compression operations. As a result of the increasing number of compression operations during the tests, much more intense lamellae fragmentation and gradual reconstruction of the microstructure were observed, which after total strain of 3.6 had a globular character

and was highly fragmented (Figures 8(e) and (f)). α phase was uniformly distributed in the β phase matrix and had a shape similar to small equiaxed and thin grains (Figure 8(f)).

D. Mechanical Properties

1. Results of the tensile tests

Tensile tests were carried out at room temperature, at a cross-head speed of 0,033 mm s^{-1}. The results of the tests are summarized in Figure 9. The application of deformation in the MaxStrain test, along with increasing its total value, led to an increase in the tensile strength. However, this impact was much more efficient in the case of the alloy obtained by the PM method. The compacts subjected to MaxStrain tests conducted with the highest total strain showed a higher tensile strength, by about 10 pct compared to the plastically processed cast alloy. For both materials in a state after heat treatment, without deformation (Figure 9(a)), similar R_m values were obtained. A large difference in the values of elongation of materials before deformation was observed. As a result of compression in the MaxStrain tests, the elongation value slightly increased (or did not change) depending on the value of the total strain. In the case of the feedstock in the form of a plastically processed cast alloy, a tendency to decrease in
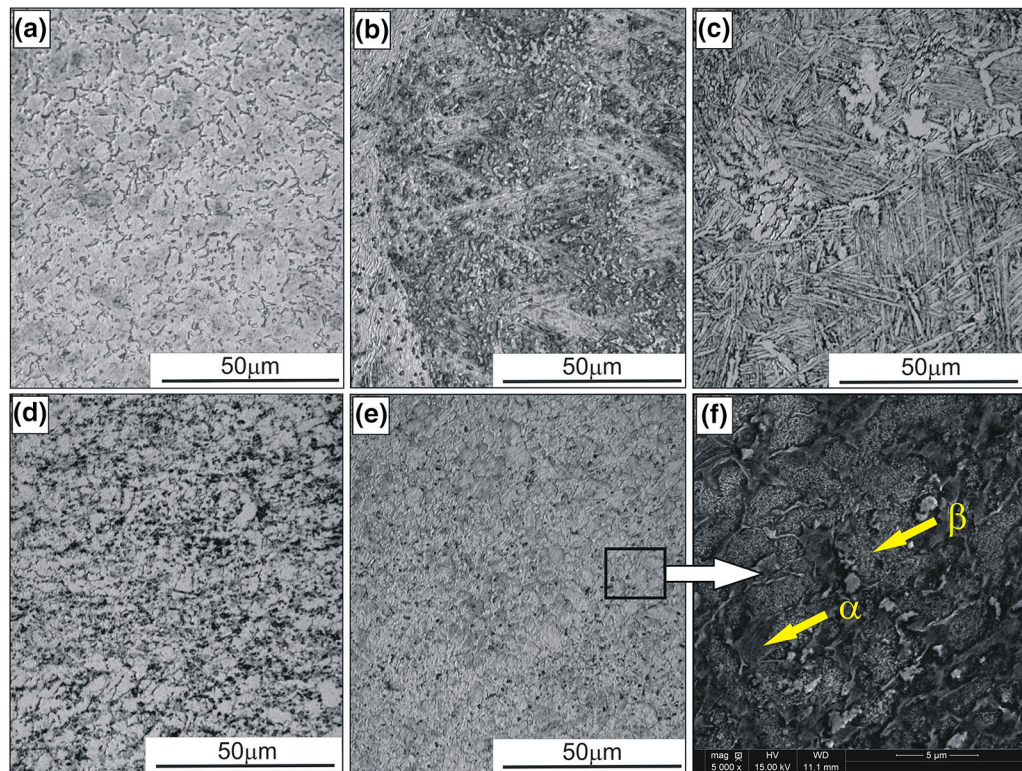
Fig. 7—The microstructure of Ti-6Al-4V alloy obtained by rolling of the cast alloy: (*a*) as-delivered cast alloy; (*b*) through (*f*) samples subjected to MaxStrain tests. Samples: (b) after initial heat treatment, undeformed (c) through (f) and after initial heat treatment and multi-axis compression with total strain of: (c) 1.5; (d) 2.4; (e, f) 3.6. Cross-sections, etched, area of observation according to Fig. 6. Observations by light microscopy (a) through (e), (f) SEM.

elongation was observed. Therefore, as the number of compression operations increased, the difference in the ductility of both materials was getting smaller (Figure 9(b)).

2. *Hardness measurements*

The measurements were carried out using the Vickers method, according to the diagram shown in Figure 6. The examples of hardness distributions obtained for the samples subjected to MaxStrain tests as well as HV_2 average values are compiled in Figure 10. The hardness of the samples subjected only to heat treatment, without deformation, was $343 \pm 10\ HV_2$ for the compact, and in the case of plastically processed cast alloy $334 \pm 4\ HV_2$. The application of deformation as well as increasing its value led to a gradual increase in the average hardness of the samples (Figure 10(d)). The hardness in the area where the accumulation of strain occurred was higher than in the non-deformed zone, which is indicated by the hardness distributions made in the A direction (Figures 10(a) through (c)). The hardness obtained for the compacts was higher than those determined for the plastically processed cast alloy, regardless of the conditions of MaxStrain tests.

The results of the research and observations carried out at this stage of the research confirmed the possibility of hot forming of PM Ti-6Al-4V alloy with the large total strain without its decohesion. The compression tests performed using the MaxStrain module led to the

fragmentation of the microstructure in both tested materials. In the case of PM samples, their multi-axis compression led to improved properties, as well.

E. *Characteristics of Hot-Rolled Ti-6Al-4V Alloy Rods*

The microstructure of PM semi-products prepared for the rolling process by the hot forging of the compacts (Figure 11) consisted of elongated or partially fragmented lamellae of the α phase as well as of the colonies of the lamellae of α and β phases located between them. The rods obtained in the hot-rolling process of the PM semi-finished products and plastically processed cast alloy were examined, and the obtained results were compared.

1. *Microstructure of the investigated materials after rolling*

The microstructure of the PM rod obtained by the hot rolling with a given total strain of 2.1 in the second stage (in four passes) consisted of fine lamellae of α and β phases and equiaxial or elongated precipitations of the α phase. The longitudinal sections of specimens observed by light microscopy showed the effect of fragmentation of massive α phase precipitates and their arrangement in bands (Figure 12(a)). Bimodal microstructure, consisting of α phase in the form of lamellae and equiaxed grains located alternately in the matrix of the β phase, was found in both observed sections of the rod, based on
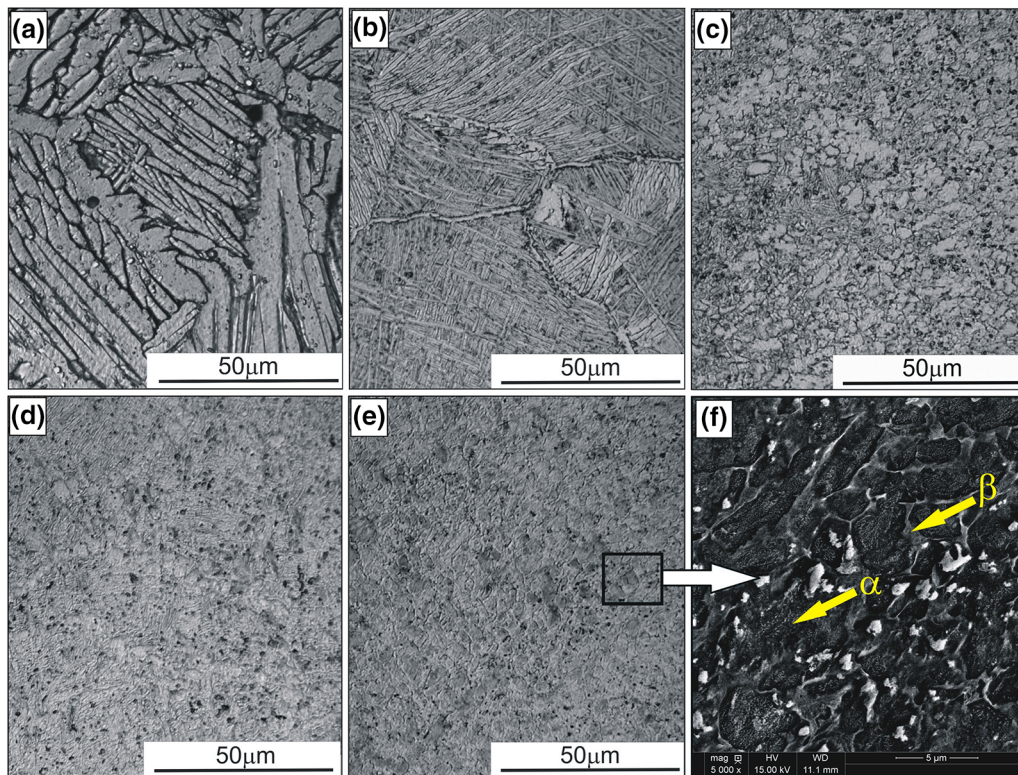
Fig. 8—Mcrostructure of Ti-6Al-4V alloy obtained by the powder metallurgy route: (*a*) alloy compact; (*b*) through (*f*) samples subjected to MaxStrain tests. Samples: (*b*) after initial heat treatment, undeformed, and (*c*) through (*f*) after initial heat treatment and multi-axis compression with a total strain of: (*c*) 1.5; (*d*) 2.4; (*e*, *f*) 3.6. Cross-sections, etched, area of observation according to Fig. 6. Observations using light microscopy (*a*) through (*e*), (*f*) SEM.
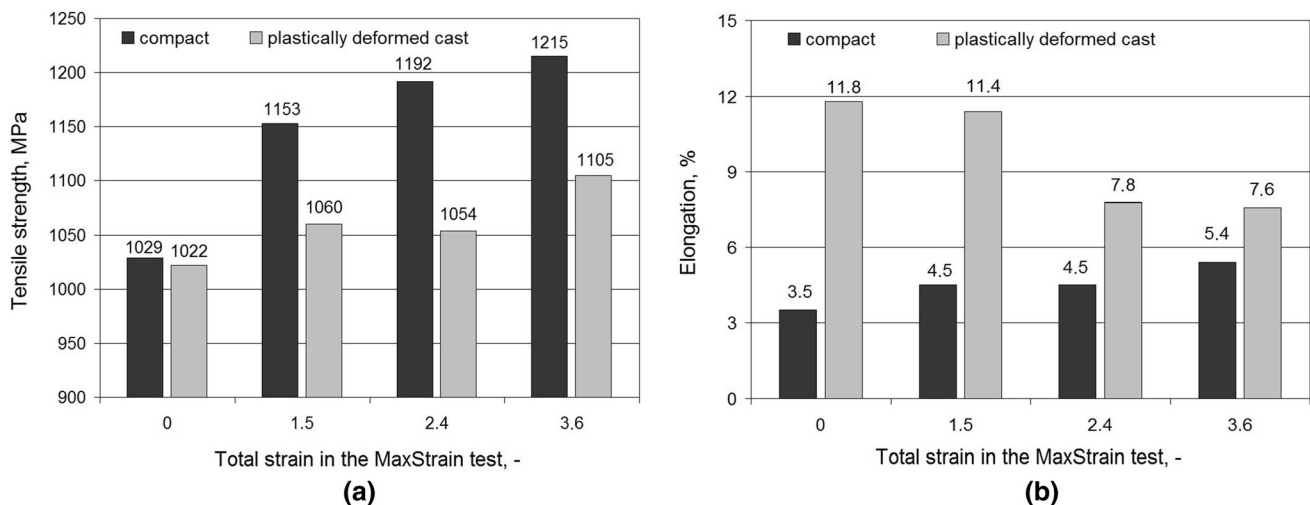
Fig. 9—Mechanical properties of the samples after MaxStrain tests: (*a*) tensile strength; (*b*) elongation.

the observation using scanning microscopy (Figures 12(b) and (d)). Increasing the total strain to about 3.5 in the second stage of rolling of PM semi-products led to the fragmentation of the microstructure (Figures 12(e) through (h)). Lamellae fragmentation was found in the areas in which small, equiaxed grains were formed. The thinner, elongated and fragmented α phase precipitates, arranged in the

direction of rolling (Figure 12(e)), were still observed. The α phase was fragmented and occurred in the β matrix in a form similar to equiaxial grains (Figures 12(f) and (h)). Apart from the last-mentioned effect, resulting from the method of deformation, changes in the microstructure of the rod in subsequent stages of the rolling process are qualitatively similar to the changes observed as a result of MaxStrain
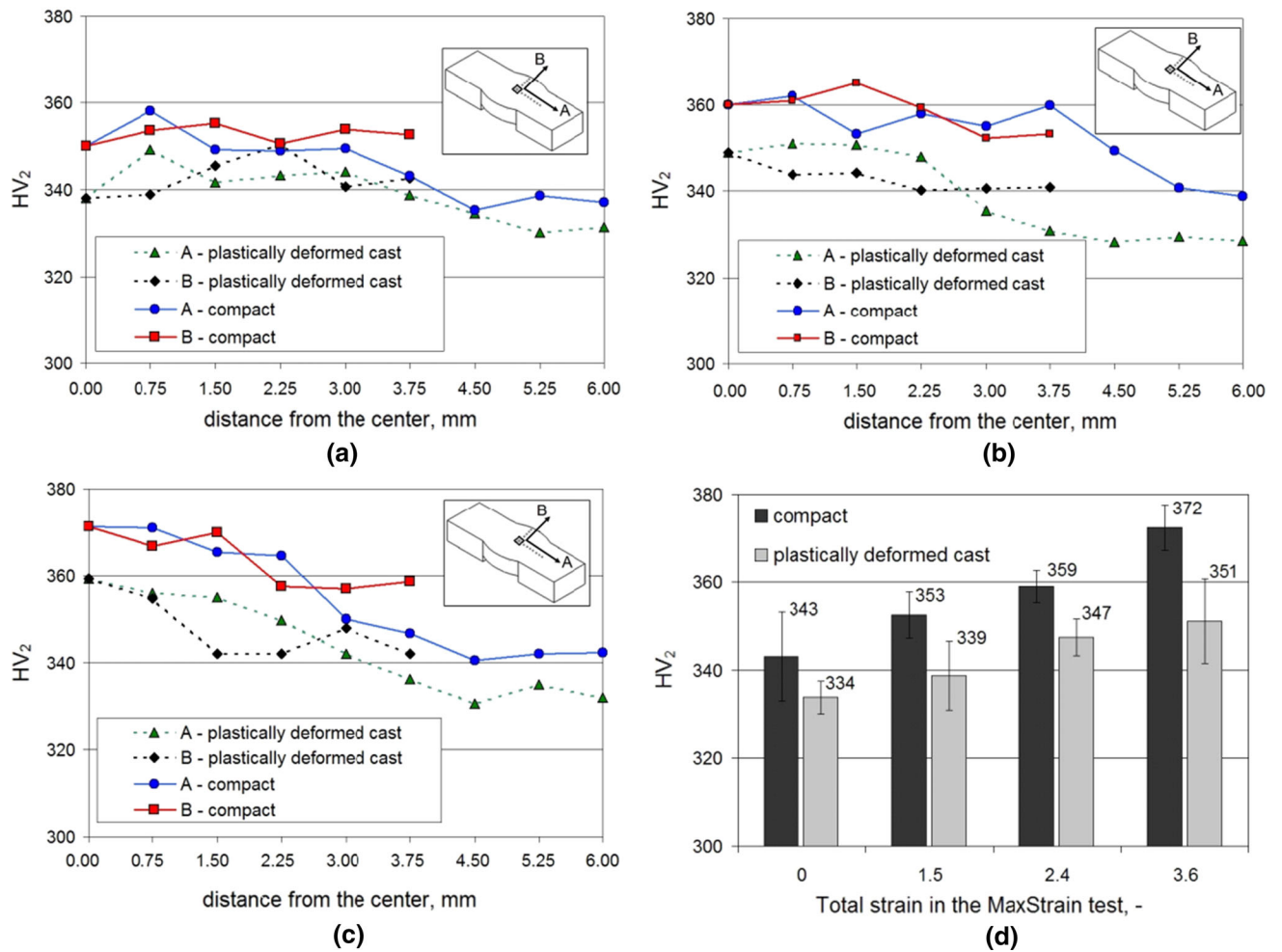
Fig. 10—Influence of the method of manufacturing of Ti-6Al-4V alloy, total deformation amount as well as the area of measurement, on the HV$_2$ hardness of the investigated alloy. Distribution of hardness in directions A and B, for a total strain during the MaxStrain test: (*a*) $\varepsilon = 1.5$; (*b*) $\varepsilon = 2.4$; (*c*) $\varepsilon = 3$; (*d*) average values of HV$_2$.
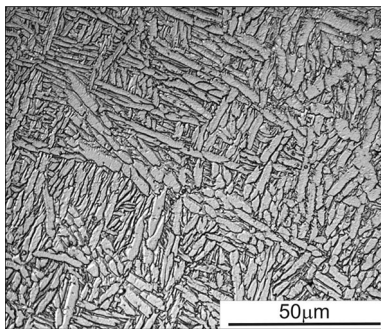

Fig. 11—Microstructure of hot forged compacts made of Ti-6Al-4V alloy. Cross-section, etched.

compression tests. Observations of the microstructure of the rod obtained from a plastically processed cast alloy (Figure 13) showed its more homogeneous and regular character compared to the microstructure of PM rods. As a result of conducting the rolling process with a total strain of 2.1, a directed arrangement of α phase precipitates was observed. Increasing the total strain in the second stage of the rolling from 2.1 to 3.5 led to a strong fragmentation of the α structure components. At this stage of the processing, the precipitates of the α phase were fragmented and shaped to the form of the equiaxed grains, uniformly distributed in the matrix of the β phase (Figures 13(e) through (h)).

2. *Hardness measurement*

Higher hardness HV$_2$ values were found in the case of rods obtained as a result of the hot rolling of PM semi-products, regardless of the amount of a total strain obtained during this process. This applies to both the hardness distributions in cross-sections (Figure 14, curves 1 to 3) and the average values evaluated based on the measurement in longitudinal sections, in the axis of rolled samples (Figure 14, points 4 and 5). For both types of feedstock, a gradual increase in hardness was observed as a result of changes in the area of measurement in the direction from the center of symmetry of the sample to its external surface. However, apart from this tendency, no significant fluctuations in hardness were observed. This also confirms the relatively small error of HV$_2$ hardness measurements taken on the longitudinal section along the axis of samples.
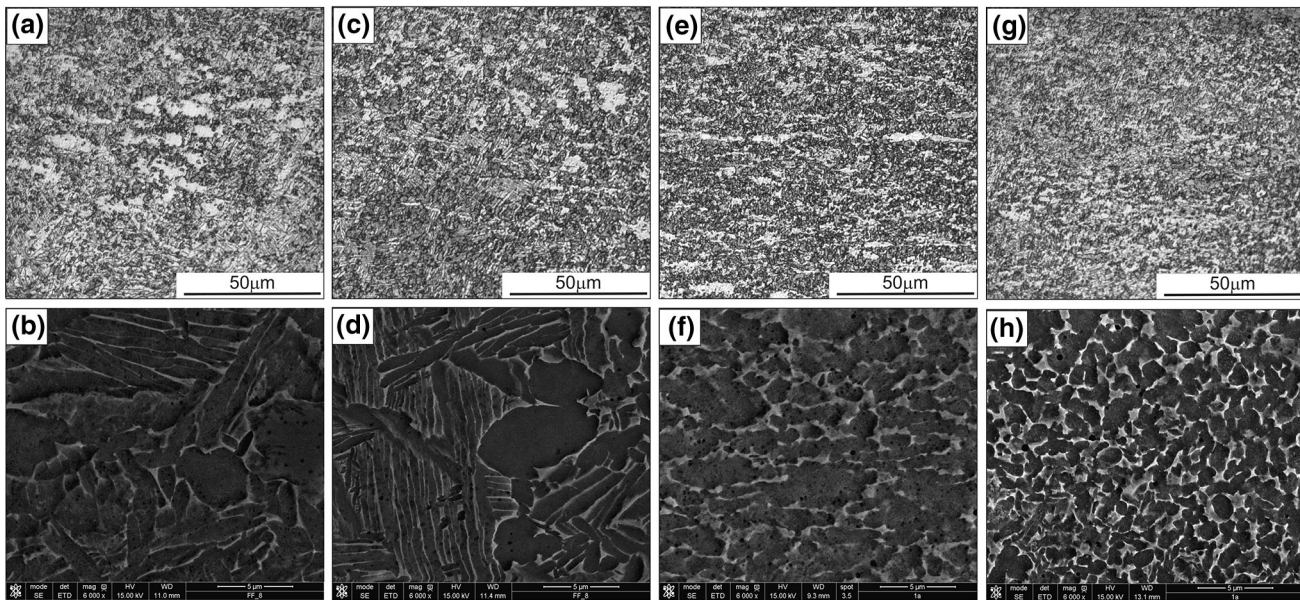
Fig. 12—Microstructure of the rod obtained in the hot rolling of the PM semi-product. Total strain: (*a*) through (*d*) 2.1; (*e*) through (*h*) 3.5. Etched sections, in the center of the sample: (a), (b), (e), (f) longitudinal section; (c), (d), (g), (h) cross-section. Observations performed with: (a), (c), (e), (g) light microscopy, (b), (d), (f), (h) SEM.
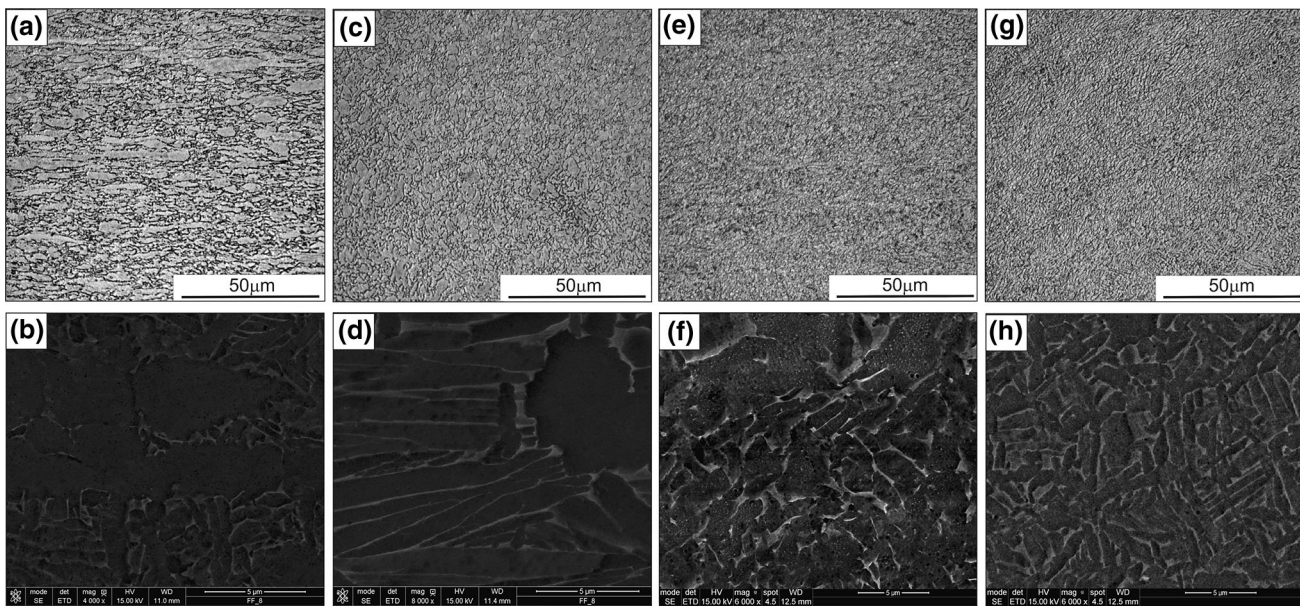

Fig. 13—Microstructure of the rod obtained in the hot rolling of the plastically processed cast alloy. Total strain of: (*a*) through (*d*) 2.1; (*e*) through (*h*) 3.5. Etched sections in the center of the sample: (a), (b), (e), (f) longitudinal section; (c), (d), (g), (h) cross-section. Observations performed with: (a), (c), (e), (g) light microscopy, (b), (d), (f), (h) SEM.

3. Tensile tests results

The characters of stress-strain curves (Figure 15) observed at the initial stage of the tensile tests performed on the compact and plastically processed cast alloy were similar. Therefore, for both of these materials, similar values of Young's modulus E, yield strength $R_{0.2}$ and tensile strength R_m were obtained. However, significantly lower ductility of the compact was observed. As a result of hot rolling, the ductility of the compact was significantly improved. In the case of the plastically processed cast alloy, no influence of this process on the obtained values of relative elongation was observed. Directional deformation applied in the hot-rolling process led to an increase of approximately 10 pct in the tensile strength of the rods obtained from both tested materials. In the case of compacts, an increase in the yield strength was also observed. The fracture surface of the compact had a brittle character, signifying trans-crystalline cracking occurring in the cross-sections of individual lamellae (Figure 16(a)). The surfaces of the
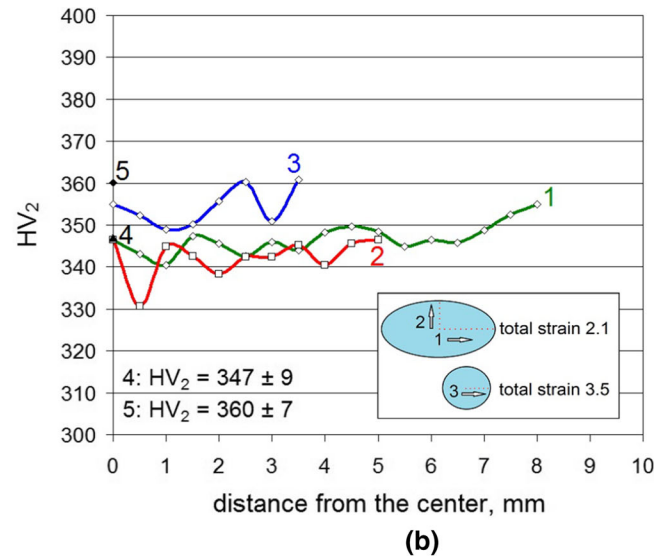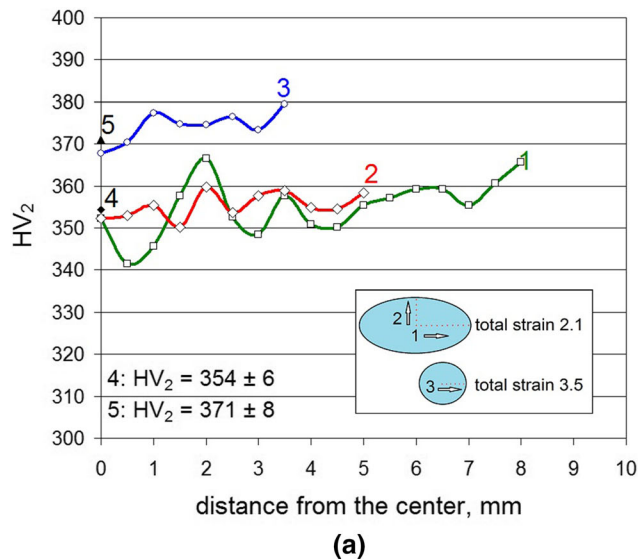
Fig. 14—HV$_2$ hardness of the alloy obtained in the rolling process: (*a*) PM semi-product; (*b*) plastically processed cast alloy. Curves (1 to 3): hardness distributions on the cross-sections, according to the scheme. Measurements 4 and 5: average HV$_2$ values based on five measurements performed on the longitudinal sections along the axis of samples rolled with a total strain of: 4 to 2.1 and 5 to 3.5.
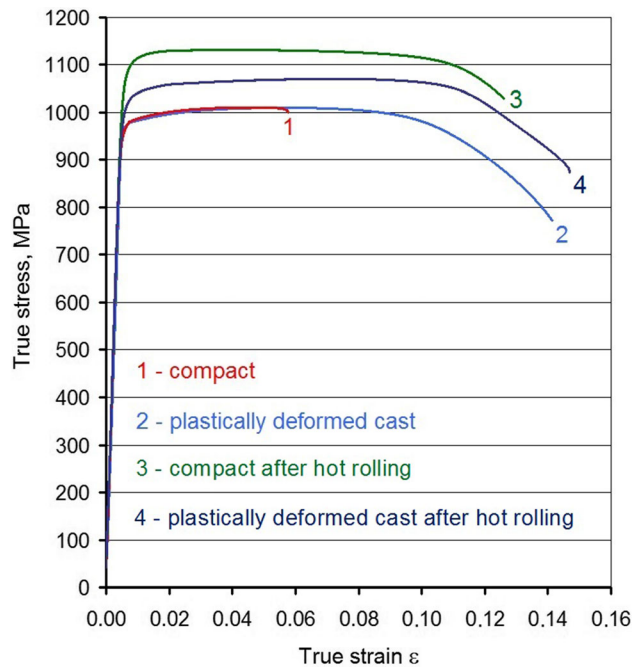

Fig. 15—Results of tensile tests of semi-products and samples after hot rolling with a total strain of 2.1.

analysis of tensile curves (Figure 15) and the results of the tensile tests (Table IV).

IV. DISCUSSION OF THE RESULTS

The research results presented in the study allowed to assess the influence of a total strain applied during multi-stage hot processing on the microstructure and selected properties of the compacts made of Ti-6Al-4V alloy as well as to compare with the results obtained for the plastically processed cast alloy tested under the same conditions. It has been shown that the semi-products produced by hot pressing of the mixture of elemental powders of titanium, aluminum and vanadium have a relative density similar to that of solid material, and its mechanical properties are comparable to those obtained for the plastically processed cast alloy. The test results and their comparison gave fundamentals to state that the properties of the Ti-6Al-4V compacts manufactured by the proposed method had properties sufficient to be used as a feedstock for processing, replacing presently used cast alloys of the same chemical composition.

It is known that many of the currently used metal forming processes, such as rolling, forging or drawing, can be carried out with large strains applied. Therefore, it was assumed that not only Ti-6Al-4V cast alloy products, but also semi-finished products manufactured using elemental powders can be manufactured applying large strains. However, this requires confirmation of the ability of PM material to deform under these conditions without decohesion as well as of the influence of total strain on the state of its microstructure and on the mechanical properties of the products.

During the MaxStrain tests the sequence of deformations is usually realized at a constant temperature, which is appropriate to obtain the grain refining effect without

fractures observed for the other materials had a ductile character (Figures 16(b) through (d)), and this type of fracture also applies to the samples made of cast Ti-6Al-4V alloy rod. The phenomenon of brittle cracking occurring at the areas of the presence of massive lamellae in the compact microstructure resulted in significantly lower elongation of this material compared to other samples, either the cast and plastically processed Ti-6Al-4V alloy or both materials after the hot-rolling process. The observations of fracture surfaces confirmed the conclusions resulting from the
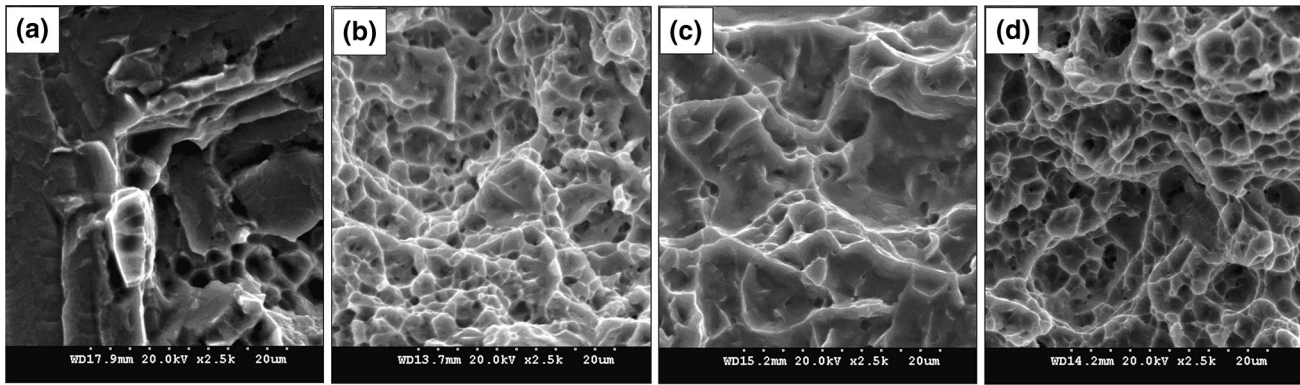
Fig. 16—Influence of the method of producing Ti-6Al-4V alloy and the state of processing on the surface of fracture resulting from the tensile test. Alloy obtained: (*a*, *b*) by PM technology; (*c*, *d*) based on the casting process. The material at initial state (b, d); after rolling with a total strain of 2.1.

Table IV.   Influence of the Stage of Processing on the Mechanical Properties of Ti-6Al-4V Alloy

State of Material	$R_{0.2}$ (MPa)	R_m (MPa)	E (GPa)	$R_{0.2}/R_m$ (Pct)	A (Pct)
Compact	950 ± 26	1022 ± 24	121 ± 16	93 ± 03	5.9 ± 0.9
Plastically Processed Cast Alloy	978 ± 18	1017 ± 22	108 ± 19	96 ± 01	13.5 ± 3.1
Compact After Hot Rolling	1056 ± 29	1122 ± 42	112 ± 10	94 ± 01	11.5 ± 5.6
Plastically Processed Cast Alloy After Rolling	975 ± 30	1064 ± 17	111 ± 07	92 ± 02	14.1 ± 3.1

the risk of decohesion of the tested material. In this work, an unusual method of performing the MaxStrain tests was applied, consisting of starting the mechanical part of the test at the temperature of 1000 °C and its realization with cooling between successive deformations allowed for the simulation of the temperature drop occurring during the processes carried out in industrial conditions. This approach allowed using the MaxStrain module as a tool for physical simulation under controlled conditions of the hot forming processes that are implemented in many single deformations and with large total strains, such as multi-pass hot rolling.

Based on the results of the MaxStrain tests, the possibility of multi-stage deformation of the compacts without decohesion of the samples was confirmed. The assessment of the quality of the samples subjected to MaxStrain tests did not reveal any defects. The impact of the testing conditions on the state of the microstructure and selected properties of the alloy obtained by powder metallurgy methods and the plastically processed cast alloy adopted as the referenced material was determined. Heat treatment conducted before the MaxStrain test for both types of deformed material at the temperature of 1000 °C (above the β-transus temperature) resulted in a change of microstructure from fine, globular grains of wrought Ti-6Al-4V alloy and massive, lamellar grains of PM material to thin lamellar grains with a small fraction of uniaxial grains (slightly more for wrought). During the hot deformation, dynamic globularization occurred.[42] Previously, this phenomenon was reported by Shell and Semiatin[43] and Warwick *et al.*[44] for hot-processed Ti-6Al-4V alloy. The first signs of the dynamic globularization appear at

the primary β grain boundaries and at the areas of breakdown and bending of the α lamellar colonies. This is because of the high amount of deformation during the process and its inhomogeneity on the α/β phase boundaries. Considering the above, the high strains promote an increase of the intensity of the dynamic globularization process resulting in the fully globularized microstructure. The crucial aspect regarding receiving the same microstructure in the case of both PM and wrought materials was heat treatment applied before deformation. The microstructure observations of the samples deformed in MaxStrain tests can be compared to the results after the hot-rolling process because of the high strains in both processes and similar temperature conditions, *i.e.*, a gradual temperature decrease during processes. The deformation as well as increasing its total value during the MaxStrain tests conducted with a simultaneous, controlled reduction of temperature led to the gradual return of the microstructure to its original state. Subjecting the compacts to heat treatment without deformation and rapid cooling immediately after the finishing of the compressions sequence led to obtaining much smaller α phase lamellae and reducing the thickness of this phase precipitation at the primary boundaries of the β grains. Applying large strains and increasing their total values led to fragmentation of the microstructure as well as its gradual rebuilding to a globular form. The microstructure of the samples subjected to total strain of 3.6 had a globular character and was highly fragmented. No significant differences in the microstructure of the compacts and plastically processed cast alloy deformed under these conditions were observed. The application of large strain, or an

increase in its total value, led to an increase in the tensile strength of the samples; however, in the case of the compacts, this effect was greater. The ductility of the PM alloy was lower. With the increase in the total strain in MaxStrain tests, a slight increase in the elongation of the compacts and a decrease in this value for the alloy obtained by casting were observed, which led to a reduction of differences in the ductility of the compared materials. Multi-axis compression resulted in increased hardness of the samples. The average HV_2 values of the compacts were higher than those determined for the plastically processed cast alloy.

The MaxStrain tests were carried out in laboratory-controlled conditions; therefore, the confirmation of their results in industrial conditions was necessary. For this purpose, hot-rolling tests were realized. As the feedstock for the rolling, both the material obtained by powder metallurgy and the plastically processed cast alloy were used. Subsequent roll passes were realized, allowing for applying total strains of about 2.1 and 3.5. These values were similar to those used in MaxStrain tests. After rolling, the samples were cooled down in air. The results of rolling tests confirmed the possibility of hot working of Ti-6Al-4V alloy compacts in industrial conditions, applying large total strains without decohesion. The microstructure of the rod obtained by rolling a compact, with the applied strain of 2.1, was composed of fine lamellae of α and β phases and massive precipitates of the α phase, which occurred in the form of bands. Rolling the compact with a total strain of about 3.5 led to the fragmentation of lamellae, in the place of which equiaxed grains of small size were created. It also led to a strong refinement of the microstructure. Elongated bands of the α phase-oriented according to the rolling direction were still observed; however, their massiveness was significantly lower.

During both the MaxStrain tests and hot-rolling process, the samples were heated up to 1000°C, which is the temperature above the β-transus for an investigated alloy. For the continuous hot-rolling process, the temperature decrease was natural. MaxStrain tests were performed to simulate similar temperature conditions during hot rolling. Therefore, the temperature decreased gradually with the increase of strain (after each deformation stage). Consequently, the $\beta \rightarrow \alpha + \beta$ transformation had to take place. It can be seen that after the first MaxStrain deformation stage (Figures 7(c), 8(c)), the microstructure had features characteristic for cooling down from the temperature above β-transus [45,46]. The massive α lamellae on the primary β grain boundaries and the colonies of thin plates within them are visible. Nevertheless, the effects of deformation, like α grain globularization, are also noticed, and they play the most significant role in the further evolution of the microstructure. However, often reported phenomena such as stress-induced precipitation of secondary α phase[47,48] were not observed under applied conditions; nevertheless, on the early stage of deformation (on the boundaries of β-phase field and $\alpha + \beta$ phase field), such phenomena might occur.

In the case of rods obtained as the result of hot rolling of compacts, higher hardness HV_2 was found compared to the material deformed in the same way obtained by casting. For both types of feedstock, a gradual increase in hardness was observed in the result of changes in the area of measurement in the direction from the center of symmetry of the bar to its external surface. The reason for this effect was faster compared to the internal zone, decreasing the temperature in the zone at the surface of the rolled bar, because of the contact with significantly cooler tools and heat exchange with the environment. Mentioned phenomena resulted in a greater strengthening of the external zone of the bars during the rolling in the subsequent deformation passes. Apart from this tendency, no significant fluctuations in hardness were observed. The selected properties of rolled materials were determined, and the obtained results were compared with those obtained from the testing of non-deformed feedstock. In the initial state, both materials had similar values of the Young's modulus, yield point and ultimate tensile strength, while the ductility of the material produced from powders was much lower. Deformation in the rolling process led to an increase in the tensile strength of both materials. In the case of compacts, the beneficial effect of their multi-stage deformation on the ductility and strength of the product was found. The surfaces of fracture resulting from the tensile tests of the bars obtained from both types of tested feedstock showed a ductile character, with no significant differences in their quality.

V. CONCLUSIONS

Based on the results of testing of Ti-6Al-4V alloy obtained by the powder metallurgy method and casting method, the scope of which included physical modeling of multi-stage deformation using the MaxStrain module as well as rolling tests, it was found that:

1. The proposed method of producing Ti-6Al-4V alloy, based on powder metallurgy technology and realized using relatively cheap elemental powders as starting materials, is suitable to form Ti-6Al-4V alloy compacts with high relative density and properties allowing their use as a feedstock for forming realized with large total strain.
2. Compression tests of Ti-6Al-4V alloy compacts using the MaxStrain module, realized with the application of large total strain and with semi-operational cooling of samples modeling industrial conditions, can be carried out without decohesion of the samples. The multi-stage deformation carried out under controlled conditions led to the significant fragmentation of the microstructure of both tested materials, which in the case of PM samples resulted in improving their properties.
3. The results of MaxStrain tests carried out in laboratory conditions were verified in industrial conditions by hot-rolling tests. In the case of PM alloy, beneficial effects of the application of multi-stage deformation and increasing its total amount on the state of microstructure and the mechanical properties of the products were found.

4. The results of the realized research extend the state of the knowledge on hot forming of the materials based on Ti-6Al-4V alloy, in particular those produced by the powder metallurgy route. They also provide the basis for the design of the processes of multi-stage working of such alloys, realized with large strains. Therefore, this knowledge should significantly contribute to the widening of their applications.

ACKNOWLEDGMENTS

OPEN ACCESS

REFERENCES

1. R. Boyer, G. Welsch, and E.W. Collings: *Materials Properties Handbook: Titanium Alloys*, 2nd ed., ASM International, Ohio, 1998.
2. G. Lütjering and J.C. Williams: *Titanium*, 2nd ed., Springer, Berlin, 2007.
3. C. Chunxiang, H. Bao Min, Z. Lichen, and L. Shuangjin: *Mater. Des.*, 2011, vol. 32, pp. 1684–91.
4. O.M. Ivasyshyn and A.V. Aleksandrov: *Mater. Sci.*, 2008, vol. 44 (3), pp. 311–27.
5. T. Saito: *JOM*, 2004, vol. 56 (5), pp. 33–36.
6. P. Mohan, A.B. Elshalakany, T.A. Osman, V. Amigo, and A. Mohamed: *J. Alloys Compd.*, 2017, vol. 729, pp. 1215–25.
7. M. Wojtaszek, T. Śleboda, A. Czulak, G. Weber, and W.A. Hufenbach: *Arch. Metall. Mater.*, 2013, vol. 58 (4), pp. 1261–65.
8. M. Wojtaszek, T. Śleboda, A. Czulak, G. Weber, W.A. Hufenbach: Met. *2014 Int. Conf. Metall. Mater. Conf. Proc.*, 2014, pp. 1405–10.
9. J. Brezinová, R. Hudák, A. Guzanová, D. Draganovská, G. Ižaríková, and J. Koncz: *Metals*, 2016, vol. 6, pp. 171–87.
10. M. Long and H.J. Rack: *Biomaterials*, 1998, vol. 19, pp. 1621–39.
11. M. Niinomi: *Mater. Sci. Eng. A*, 1998, vol. 243, pp. 231–36.
12. J. Shi, J. Yang, Z. Li, L. Zhu, L. Li, and X. Wang: *J. Alloys Compd.*, 2017, vol. 728, pp. 1043–48.
13. A. Cuadrado, A. Yánez, O. Martel, S. Deviaene, and D. Monopoli: *Mater. Des.*, 2017, vol. 135, pp. 309–18.
14. S. Yan-Wei, G. Zhi-Meng, H. Jun-Jie, and Y. Dong-Hua: *Procedia Eng.*, 2012, vol. 36, pp. 299–306.
15. P. Heinl, L. Müller, C. Körner, R.F. Singer, and F.A. Müller: *Acta Biomater.*, 2008, vol. 4, pp. 1536–44.
16. K. Wang: *Mater. Sci. Eng. A*, 1996, vol. 213, pp. 134–37.
17. L. Bolzoni, E.M. Ruiz-Navas, and E. Gordo: *Mater. Des.*, 2013, vol. 52, pp. 888–95.
18. A. Carman, L.C. Zhang, O.M. Ivasishin, D.G. Savvakin, M.V. Matviychuk, and E.V. Pereloma: *Mater. Sci. Eng. A*, 2011, vol. 528, pp. 1686–93.
19. C. Haase, R. Lapovok, H.P. Ng, and Y. Estrin: *Mater. Sci. Eng. A*, 2012, vol. 550, pp. 263–72.
20. L. Bolzoni, I. Montealegre Meléndez, E.M. Ruiz-Navas, and E. Gordo: *Mater. Sci. Eng. A*, 2012, vol. 546, pp. 189–97.
21. D.L. Zhang, S. Raynova, V. Nadakuduru, P. Cao, B. Gabbitas, and B. Robinson: *Mater. Sci. Forum*, 2009, vols. 618–619, pp. 513–16.
22. V.S. Moxson, O.N. Senkov, and F.H. Froes: Production and applications of low cost titanium powder products*Int. J. Powder Metall.*, 1998, vol. 34 (5), pp. 45–53.
23. S.L. Semiatin, N.C. Levkulich, C.A. Heck, A.E. Mann, N. Bozzolo, A.L. Pilchak, and J.S. Tiley: *Metall. Mater. Trans. A Phys. Metall. Mater. Sci.*, 2020, vol. 51, pp. 2291–2305.
24. Y.C. Lin, Q. Wu, G.D. Pang, X.Y. Jiang, and D.G. He: *Adv. Eng. Mater.*, 2020, vol. 22, p. 1901193.
25. Y.C. Lin, Y.W. Xiao, Y.Q. Jiang, G.D. Pang, H.B. Li, X.Y. Zhang, and K.C. Zhou: *Mater. Sci. Eng. A*, 2020, vol. 782, p. 139282.
26. J.W. Qiu, Y. Liu, B. Liu, Y.B. Liu, B. Wang, R. Earle, and H.P. Tang: *J. Mater. Sci.*, 2012, vol. 47, pp. 3837–48.
27. X. Xu, P. Nash, C. Li, P. Nash, D. Mangabhai, and W. Lu: *J. Mater. Res.*, 2015, vol. 30 (8), pp. 1056–64.
28. O. Kanou, N. Fukada, and M. Hayakawa: *Mater. Trans. JIM*, 2016, vol. 57 (5), pp. 681–85.
29. C. Liang, M.X. Ma, M.T. Jia, S. Raynova, J.Q. Yan, and D.L. Zhang: *Mater. Sci. Eng. A*, 2014, vol. 619, pp. 290–99.
30. F. Yang, D. Zhang, B. Gabbitas, H. Lu, and C. Wang: *Mater. Sci. Eng. A*, 2014, vol. 598, pp. 360–67.
31. M. Jia, D. Zhang, J. Liang, and B. Gabbitas: *Metall. Trans. A*, 2017, vol. 48, pp. 2015–29.
32. O.M. Ivasishin, D.G. Savvakin, V.S. Moxson, K.A. Bondareval, and F.H. Froes: *Mater. Technol.*, 2002, vol. 17 (1), pp. 20–25.
33. S.M. El-Soudani, K. Yu, E.M. Crist, F. Sun, M.B. Campbel, T.S. Esposito, J.J. Phillips, V. Moxson, and V.A. Duz: *Metall. Trans. A*, 2013, vol. 44, pp. 890–910.
34. I. Khmelevskaya, V. Komarov, R. Kawalla, S. Prokoshkin, and G. Korpała: *J. Mater. Eng. Perform.*, 2017, vol. 26, pp. 4011–19.
35. I. Khmelevskaya, V. Komarov, R. Kawalla, S. Prokoshkin, and G. Korpała: *Mater. Today.: Proc.*, 2017, vol. 4, pp. 4830–35.
36. J. Majta and K. Muszka: *Mater. Sci. Eng. A*, 2007, vol. 464, pp. 186–91.
37. P. Bereczki, V. Szombathelyi, and G. Krállics: *Int. J. Mech. Sci.*, 2014, vol. 84, pp. 182–88.
38. J.W. Adams, V.A. Duz, V.S. Moxson, W.R. Roy: Low Cost Blended Elemental Titanium Powder Metallurgy. Conference Materials: Titanium 2007, October 7–9, Orlando, Florida, 2007.
39. F.H. Froes:Powder metallurgy of titanium alloys in *Advances in Powder Metallurgy: Properties, Processing and Applications*, W.I. Chang and Y. Zhao, eds., Woodhead Publishing Limited, Cambridge, 2013, pp. 202–40.
40. G. Cantin, N. Stone, D. Alexander, M. Gibson, D. Ritchie, R. Wilson, M. Yousuff, R. Rajakumar, and K. Rogers: *Mater. Sci. Forum*, 2010, vols. 654–656, pp. 807–10.
41. O.M. Ivasishin, D. Eylon, V.I. Bondarchuk, and D.G. Savvakin: *Book Series: Defect and Diffusion Forum*, Trans Tech Publications, Zurich, 2008, vol. 277, pp. 177–85.

42. Y.Q. Jiang, Y.C. Lin, X.Y. Jiang, D.G. He, X.Y. Zhang, and N. Kotkunde: *Mater. Character.*, 2020, vol. 163, p. 110272.
43. E.B. Shell and S.L. Semiatin: *Metall. Mater. Trans. A*, 1999, vol. 30A, pp. 3219–29.
44. J.L.W. Warwick, N.G. Jones, I. Bantounas, M. Preuss, and D. Dye: *Acta Mater.*, 2013, vol. 61, pp. 1603–15.
45. S.L. Semiatin: *Metall. Mater. Trans. A*, 2020, vol. 51A, pp. 2593–2625.
46. Y.C. Lin, Y. Tang, Y.Q. Jiang, J. Chen, D. Wang, and D.G. He: *Adv. Eng. Mater.*, 2020, vol. 22, p. 01901436.
47. F. Sun, J.Y. Zhang, M. Marteleur, T. Gloriant, P. Vermaut, D. Laillé, P. Castany, C. Curfs, P.J. Jacques, and F. Prima: *Acta Mater.*, 2013, vol. 61, pp. 6406–17.
48. M. Bignon, E. Bertrand, F. Tancret, and P.E.J. Rivera-Díaz-del-Castillo: *Materialia*, 2019, vol. 7, p. 100382.